Desalination 474 (2020) 114189

Contents lists available at ScienceDirect

Desalination

journal homepage: www.elsevier.com/locate/desal

Analysis of the energy consumption of supercritical water desalination (SCWD)

Surika van Wyk[a,b], Aloijsius G.J. van der Ham[a], Sascha R.A. Kersten[a,*]

[a] Sustainable Process Technology, Faculty of Science and Technology, University of Twente, Postbus 217, 7500 AE Enschede, the Netherlands
[b] Wetsus, European Center of Excellence for Sustainable Water Technology, Oostergoweg 9, 8911 MA Leeuwarden, the Netherlands

ARTICLE INFO

Keywords:
Supercritical water desalination (SCWD)
Process modelling
Thermodynamics
Pilot plant validation

ABSTRACT

An experimental and modelling study was done to investigate supercritical water desalination (SCWD) with respect to energy consumption as a function of the NaCl concentration (0 to 20 wt%). Pilot plant experiments were performed for different flow rates and feed concentrations, and used for the validation of the thermodynamic models (eNRTL and Anderko & Pitzer) employed for phase equilibria and enthalpy calculations. Experimental and modelling results showed that the lowered heat capacity of the feed streams, while increasing the concentration from 0 to 7 wt%, leads to improved performance of the feed - supercritical water (SCW) heat exchanger (HEX), evident from a higher feed outlet temperature. For concentrations of ≥14 wt%, pre-heating of the feed, prior to the HEX, is recommended due to the decrease in the SCW recovery in the SCW-brine separator. The calculated duty, of the heater bringing the heat-exchanged feed to the separation temperature, decreases with NaCl concentration due to the decrease in the feed heat capacity. The calculated overall energy consumption of SCWD was between 0.71 and 0.90 MJ_{th}/kg_{feed}. For higher concentration feeds, the energy input is divided between low – and high quality (temperature) heat.

1. Introduction

Brine management has gained increased attention in the past few years due to the growing demand for fresh drinking water and the accompanying increased brine production. According to Jones et al. [1], the global desalinated water production is 95.4 million m^3/day, while the brine production is 141.5 million m^3/day. Almost 50% of the brine producing plants are located less than one kilometre from the coastline and in most cases brine waste is discharged into the oceans. However recently, more stringent regulations are being put into effect to prevent the discharge of waste brine streams into the oceans and lakes, which is already threatening the ecosystem and marine life [2–5]. The demand for zero liquid discharge (ZLD) technology is, therefore, increasing as new methods need to be developed for the treatment of brine streams.

Supercritical water desalination (SCWD) is a ZLD technology that utilises the non-polar nature of water under supercritical conditions (Temperature > 374 °C, Pressure > 22.1 MPa) to separate salt from water. This approach to desalination has been investigated for the treatment of seawater and more concentrated waste brine streams (≥3.5 wt% NaCl) [6–8]. Under supercritical conditions, the properties of water start to change significantly, causing the water to become non-polar in nature. Consequently, the solubility of inorganics — such as salt — in water decreases and inorganics can be easily separated from water [9–11]. The phase behaviour and removal of different salts from supercritical water (SCW) has been extensively studied using various laboratory scale set-ups [12–18] and recently pilot plant scale facilities have been built and tested [6–8].

The advantage of this technology, over conventional desalination processes, is that it is robust (extensive pre-treatment is not required) and is applicable to different brine streams with varying concentrations. Depending on the separation conditions, the recovery of drinking water can be up to 93% (mass basis) for a feed concentration of 3.5 wt% NaCl. A major drawback is, however, that the process is energy intensive. In their conceptual design of the SCWD process, Odu et al. [18] estimated the thermal energy requirement to be 450 MJ_{th}/m^3 drinking water for a 3.5 wt% NaCl feed. In this section, the thermal energy only refers to the energy required to heat the feed to the separation temperature (after heat integration) and for the separation itself, no other thermal energy requirements (*e.g.* cooling) of the process are considered. Lopez & Trembly [7] simulated a SCWD unit with pre-treatment (chemical pre-treatment to reduce the concentration of scale forming salts) and estimated the thermal energy requirement to be between 647 and 726 MJ_{th}/m^3_{feed}. In a later study, Ogden & Trembly [8] experimentally determined the thermal energy requirement to be between 178 and

* Corresponding author.
E-mail address: s.r.a.kersten@utwente.nl (S.R.A. Kersten).

https://doi.org/10.1016/j.desal.2019.114189
Received 2 August 2019; Received in revised form 18 October 2019; Accepted 18 October 2019
Available online 30 October 2019

495 kJ/kg, depending on feed concentration and separation pressure. For conventional desalination processes, the energy consumption is much lower, at 30 $MJ_{el}/m^3_{drinking\ water}$ for seawater reverse osmosis and 300 $MJ_{th}/m^3_{drinking\ water}$ for multi-stage flash, but they are not ZLD technologies, producing a concentrated brine waste [19].

For the above mentioned SCWD studies, the energy required to heat the feed to the desired separation temperature was the main contributor to the overall energy consumption of the SCWD process. Reducing the heating requirement should thus be the main target for reducing the overall energy consumption of the unit. Steps have already been taken by utilising the heat from the produced SCW to heat the feed [6]. Another manner in which the energy consumption can be decreased is by increasing the salt concentration of the feed. Salt has a lower heat capacity compared to that of water, with the heat capacity of NaCl being 0.88 kJ/kg K [20] and that of water 4.19 kJ/kg K [21] at 25 °C and 1 bar. Lowering the heat capacity of the feed could result in lowering the energy required to heat the feed to supercritical conditions. There are, however, drawbacks to increasing feed concentration such as lowering the SCW recovery, which could alter the heat exchange potential. The aim of this work was to investigate the energy requirement (specifically the feed heater, see Fig. 1) of SCWD, as a function of the NaCl concentration of the feed. The research approach was based on experiments performed on a pilot plant scale SCWD unit and process modelling. To support the latter a thorough validation (experimental and literature based) was done of the thermodynamic model used to calculate the properties in the supercritical section of the unit.

2. SCWD process

The proposed layout of SCWD unit with ZLD and phase separation is shown in Fig. 1.

The SCWD process can be divided into three main sections, namely the heating section consisting of a heat exchanger (HEX) and a heater, the gravity separator and the brine recovery units (ZLD units). For our proposed SCWD scheme, a saline feed (#1) was firstly pressurised and then heated in a counter-current HEX using the supercritical water (SCW) outlet stream (#5) as the hot fluid. To ensure the desired separation temperature was reached additional heat was provided by the heater, before the stream entered the separator. Inside the gravity separator, the SCW phase (500–700 ppm NaCl) was separated from the concentrated hydrothermal brine phase (#8; 30–50 wt% NaCl) as shown in the phase diagram. The concentrated brine accumulated in the gravity separator up to a certain level, while the SCW was continuously removed. Afterwards the brine was rapidly expanded into the brine recovery units by opening the high-pressure, high-temperature valve.

In our previous work [6], the detailed operation and first results of a SCWD pilot plant for feeds of 3–16 wt% NaCl were presented. For the pilot plant experiments, the brine expansion only occurred in one step (1st stage flash), however, experimental results and calculations showed that a one-step expansion was not sufficient in obtaining ZLD. Based on theoretical calculations, a two-step separation scheme was proposed, in which an additional flash-evaporation step was added to further dry the salts [6].

3. Thermodynamics and validation

The modelling of the SCWD unit was divided into two sections, namely the supercritical and subcritical section. The supercritical section included the cold outlet (stream #3 – Fig. 1) and hot inlet (#5) stream of the HEX, as well as the separator feed (#4) and the concentrated brine (#8). The subcritical section covers the feed stream (#1), cold inlet (#2) and hot outlet (#6) streams of the HEX, together with the brine recovery section streams (#9–#14).

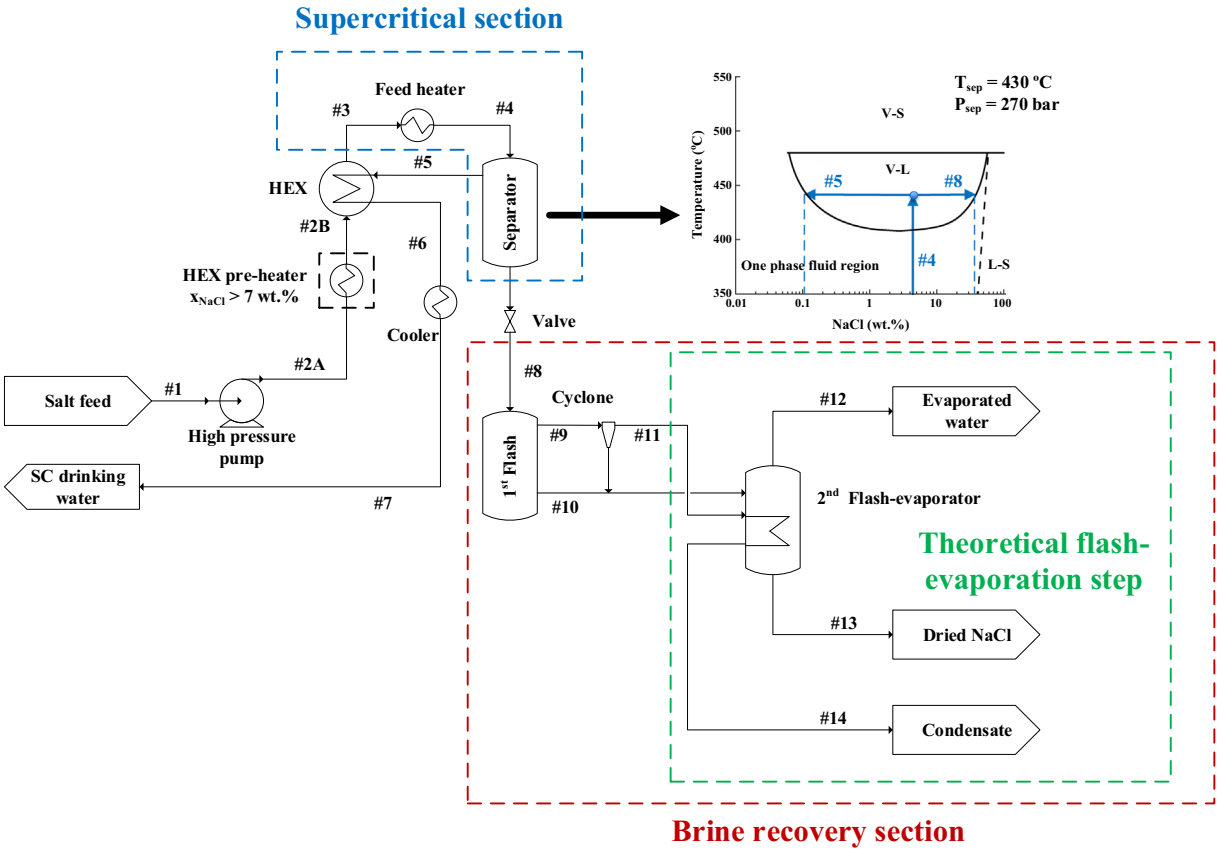

Fig. 1. SCWD with ZLD theoretical scheme.

3.1. Supercritical section

The supercritical section was modelled using the equation of state (EoS) developed by Anderko & Pitzer (AP) [22]. This EoS is a Helmholtz free energy-based model that calculates the residual Helmholtz free energy of the system, with the ideal gas state adopted as the standard state for all components. The AP EoS assumes complete electron pairing. Therefore, the process was modelled as a two-component system, consisting of NaCl (1) and H_2O (2). This assumption was made based on the significant decrease of the dielectric constant of water under supercritical conditions, which will lead to the re-association of the ions to form NaCl [22]. The AP EoS consists of two parts, namely the reference and perturbation parts, with the reference part divided into the repulsive and dipolar contributions. The equation for the residual molar Helmholtz free energy is given as follow [22]:

$$a^{res}(T,v,X) = a^{rep}(v,X) + a^{dip}(T,v,X) + a^{per}(T,v,X) \tag{1}$$

The repulsive contribution was described by the hard-sphere mixture free energy model and the dipolar contribution was calculated as the difference between the molar Helmholtz free energy of the dipolar hard spheres and that of the simple hard spheres. The perturbation part, which accounts for the deviations from the reference part, was described by an empirically fitted truncated virial-type expansion. For the pure and binary interaction coefficients of NaCl and water (included in the perturbation part), the values reported by Kosinski & Anderko [23] were used. These parameters have also been used for calculating the thermodynamic properties of supercritical water oxidation [24,25] and for verifying the empirical correlations reported by Driesner [26,27]. All detailed equations and information can be found in [22].

The specific enthalpy of a supercritical stream was calculated as the sum of the pure component enthalpies and the non-ideal mixing (excess) enthalpy:

$$h_{SC} = \sum_i X_i h_i + h_{SC}^{ex} \qquad i = NaCl,\ H_2O \tag{2}$$

For water, the pure component enthalpy was obtained from the International Association for Properties of Water and Steam Industrial Formulation 1997 (IAPWS IF-97) steam tables (Matlab XSteam) [21]. The enthalpy of NaCl was determined by integrating the isobaric heat capacity correlation fitted by Driesner [27]. The correlation was obtained from fitted isobaric heat capacity data [28] and calculated enthalpies from a standard thermodynamic expression (heat capacities were then calculated from the temperature derivative). The non-ideal mixing (excess) enthalpy was determined from the AP EoS using Eq. (3), which was derived from the Gibbs free energy equation [27,29]:

$$\left(\frac{\partial h_{SC}^{ex}}{\partial X_{NaCl}}\right)_{PT} = \left[T\left(\frac{\partial P}{\partial T}\right)_{vX} - \frac{1}{\kappa_{TX}}\right]\left(\frac{\partial v}{\partial X_{NaCl}}\right)_{PT} \tag{3}$$

All partial derivatives of Eq. (3) were determined numerically, applying the central difference method. The excess molar enthalpy was then calculated by numerically integrating (trapezoidal rule) Eq. (3) from pure water ($X_{NaCl} = 0$) to the molar salt concentration of the solution (X_{NaCl}). The numerical errors made during differentiation (interval of 0.0001) and integration (interval of 0.001) were minimal (decreased with a decrease in NaCl concentration) and had a negligible effect on the calculation results. The maximum error values (20 wt% NaCl solution) can be found in the supporting information (SI).

3.2. Subcritical section

The subcritical section was modelled using the symmetric reference state, electrolyte non-random two liquid (eNRTL) activity coefficient model developed by Song & Chen [30], which utilises a hypothetical pure fused salt reference state for the calculation of the activity coefficients for the ions, instead of the conventional infinite dilution reference state. Yan & Chen [31] modelled the thermodynamic properties of a NaCl-Na_2SO_4-H_2O mixture extensively and fitted the interaction parameters for the model for temperatures up to 200 °C and concentrations up to saturation (± 26 wt% NaCl at ambient conditions). The validated interaction parameters determined in that paper were used for this study.

To ensure unity with regards to the specific enthalpy calculations, the enthalpy was calculated as the sum of the pure component enthalpies at the system temperature and pressure and the excess enthalpy (the same as for the supercritical section). The excess enthalpy was calculated from the activity coefficients determined from the eNRTL equation, assuming complete dissociation of the ions. The dissociation enthalpy of NaCl is added to account for the ideal mixing term being the associated NaCl and not the ions. The specific enthalpy for the subcritical streams was calculated as follow:

$$h_{sub} = \sum_i X_i h_i + X_{NaCl}\Delta H_{diss} + h_{sub}^{ex} \qquad i = NaCl,\ H_2O \tag{4}$$

With:

$$h_{sub}^{ex} = -RT^2 \sum_k X_k \frac{\partial \ln \gamma_k}{\partial T} \qquad k = Na^+,\ Cl^-,\ H_2O \tag{5}$$

For the dissociation enthalpy

$$\Delta H_{diss}(T) = \Delta H_{diss}(T^{ref}) + \Delta C_{p,diss}(T - T^{ref}) \tag{6}$$

The dissociation enthalpy is −3.8 kJ/mol and the dissociation heat capacity is −0.13 kJ/mol/K at 25 °C [20]. The contribution of dissociation was minimal, being below 6% of the specific enthalpy for a feed of 20 wt% (effect of dissociation would be highest for higher feed concentrations) in the temperature range 25–300 °C. Originally, the model was fitted for 25–200 °C, however, since Yan & Chen [31] also fitted caloric data such as dissolution enthalpy, liquid enthalpy and heat capacity, the temperature dependence of the model was adequately accounted for and reliable results could still be obtained outside the temperature range of the fitted data [20]. For this study, the enthalpy calculations were performed up to a temperature of 300 °C. The specific enthalpies for 0.068, 3.5, 7.0, 16 and 20 wt% NaCl solutions were compared with the results of the Driesner correlations [27] for a temperature range of 20 to 300 °C and a constant pressure of 270 bar, with the maximum deviation being 5%. The comparison can be seen in the SI (Fig. S.5).

3.3. Validation

Validation of the modelling was done for the condition range of interest, namely 300 to 500 °C, 1 to 300 bar and compositions of 0 to 50 wt% NaCl, using various data sets found in literature as well as experimental pilot plant data. In the SI, the comparison with literature data for vapour-liquid equilibrium (VLE) and density can be found. For validation with the experimental data of our pilot plant the SCW NaCl concentration (0 to 7.0 wt%) and recoveries (both directly measured) were compared. Experiments were performed for a separation temperature and pressure of 430 °C and 270 bar so the concentration did not vary greatly, however, the recovery did change due to differences in the feed concentration. The equations for the composition and recovery are given in the SI. The parity plots for the concentration and recovery are given in Fig. 2 a & b.

The results show that the AP EoS is able to predict both the SCW concentration and recovery within an accuracy of 10 and 5%, respectively. The validation of the specific enthalpy calculations was more challenging due to literature data being mostly available in the form of calculated data by previously developed EoS, such as those by Tanger & Pitzer [32] and Bischoff & Rosenbauer [33] or in the form of empirical correlations such as those by Driesner [27] and Palliser & McKibbin [34]. In the SI, the comparison of the specific enthalpy with other EoS

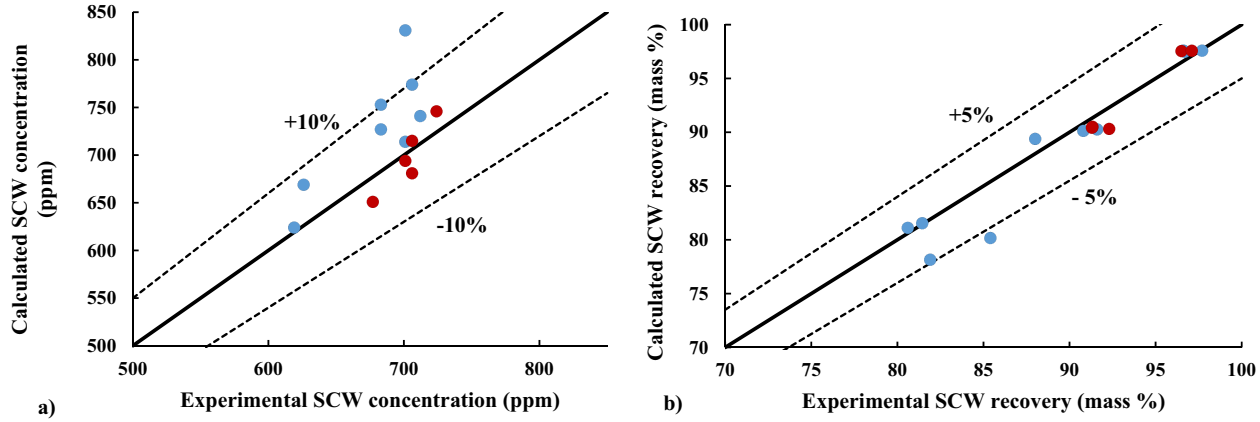

Fig. 2. Parity plot comparison of SCW a) composition and b) recovery (● 2 kg/h feed rate; ● 5 kg/h feed rate).

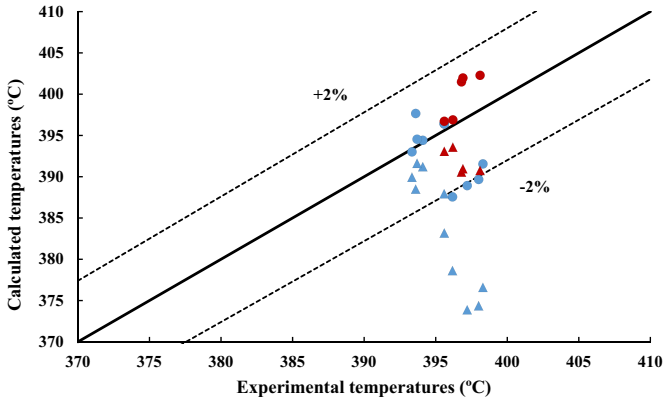

Fig. 3. Parity plot for HEX cold (Feed) outlet temperatures (● 2 kg/h – AP EoS; ● 5 kg/h – AP EoS; ▲ 2 kg/h – Ideal mixing; ▲ 5 kg/h – Ideal mixing).

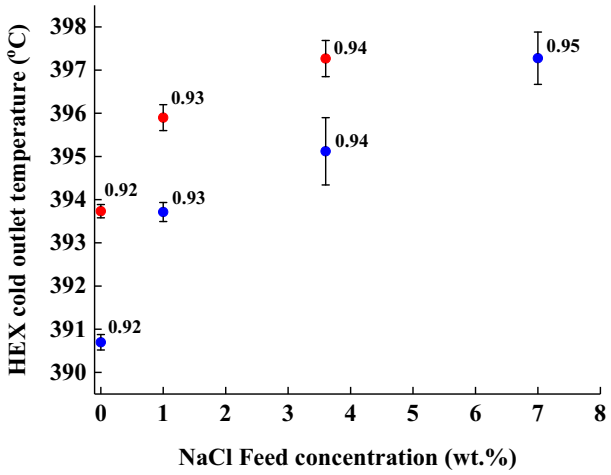

Fig. 4. Experimental HEX cold (feed) outlet temperatures for two feed rates as a function of feed concentration. Separator temperature ($T_{hot,out}$) set-point was 430 °C (● 2 kg/h; ● 5 kg/h; values reported in graph - $T_{cold,out}/T_{hot,in}$).

and correlations is given, however, this is not a validation. In order to have an indication that the AP EoS determined enthalpies are correct the HEX cold outlet temperature was calculated by performing an energy balance over the HEX and using the AP EoS to calculate the enthalpy (calculation procedure provided in the SI). The results were compared with temperatures calculated assuming ideal mixing (only the pure component enthalpies are summed) to assess the accuracy of the non-ideal mixing enthalpy calculated from the AP EoS. The heat loss of the HEX was determined from the pure water runs and the steam tables (IAPWS IF-97) by calculating the difference between the hot and cold stream duty. The heat loss was 0.92 MJ/h for a 2 kg/h feed and 1.81 MJ/h for a 5 kg/h feed and was assumed to be constant for all concentrations. The parity plot is given in Fig. 3.

TThe results show that the AP EoS is able to predict the temperatures within a 2% deviation from the experimental results. For the ideal mixing calculations, the deviations from experimental results are greater and the temperature is consistently under-predicted, especially for 2 kg/h. This is a strong indication that the enthalpies calculated for the AP EoS are more accurate in comparison to an ideal mixing approach.

4. Experimental results

Pilot plant experiments were performed for feed flow rates of 2 (0, 1.0, 3.6 and 7.0 wt% NaCl feed) and 5 kg/h (0, 1.0 and 3.6 wt% NaCl feed) respectively. Higher feed concentrations could not be used as brine accumulation was too rapid for steady state conditions to be reached. All experiments were performed for a separation temperature and pressure of 430 ± 1 °C and 270 ± 2 bar, respectively. The HEX results are summarised in Table S.3 in the SI. The HEX cold outlet temperatures for feed rates 2 and 5 kg/h are compared in Fig. 4 for different feed concentrations.

FFor varying feed rates, the absolute cold outlet temperatures are higher, however, the ratio between the cold outlet and hot inlet temperature (values given in Fig. 4) remain the same. Thus, the feed rate does not increase the HEX cold outlet temperatures for the performed experiments. The ratios for 2 and 5 kg/h are the same due to the high heat transfer effectiveness (~99%) of the pilot plant HEX, as seen from Table S.3 in the SI. The temperatures and ratios, however, do increase with NaCl feed concentration. As the feed concentration increases, the heat capacity of the feed stream decreases as well as the SCW recovery. These two occurrences have an opposing effect. A decrease in heat capacity of the cold stream will improve heat exchange potential, in that less energy is required for heating the feed, however, a decrease in the SCW recovery will result in less energy available for heat exchange. From the experimental results it can be seen that for feed concentrations 1.0 to 7.0 wt% NaCl, the decrease in the heat capacity will have the governing effect as the HEX cold outlet temperature increases. For higher feed concentrations, the effect of decreased SCW recovery will become significant and the heat exchange potential will be less (refer to Section 5.2).

To further elaborate on the effect of lowered heat capacity, the composite curves for pure water and 7.0 wt% NaCl are compared in Fig. 5. The cold curve was shifted so that a minimum temperature difference of 10 °C is maintained at the pinch point. Both curves were extended to 430 °C (set-point of the feed heater) and the measured cold

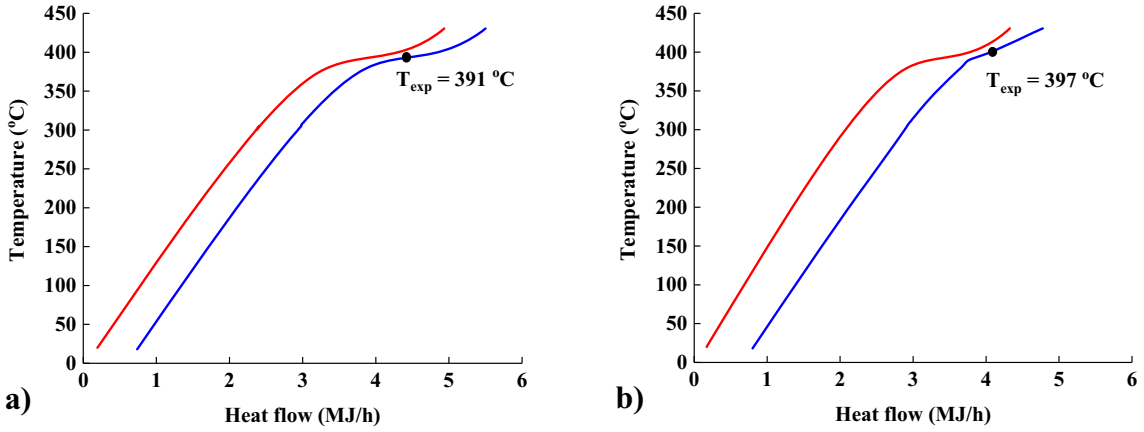

Fig. 5. Hot and cold composite curves for 2 kg/h feed at 270 bar a) pure water b) 7.0 wt% NaCl feed (■ Hot stream (SCW); ■ Cold stream (Feed); ● HEX experimental cold outlet temperature).

outlet temperature is indicated with the black dot.

For pure water the pinch point is reached in the temperature transition region around the pseudocritical point (for 270 bar the pseudocritical temperature of water is 391 °C). In this region heat exchange becomes less, due to the decrease in ΔT between the hot and cold stream. As the NaCl feed concentration increases the critical point of the feed stream shifts to a higher temperature (pseudocritical temperature is ± 410 °C for 7 wt% NaCl) and the energy required to reach the supercritical state decreases due to the heat capacity of NaCl being lower than that of water. Consequently, 1) the plateau area for the feed decreases and becomes steeper and 2) the pinch point temperature increases. These two factors assist with heat exchange potential between the streams and higher cold outlet temperatures are achieved.

5. Modelling results

5.1. SCWD process calculations

In Fig. 6, an overview of the process is given along with the corresponding equations and models used for the calculation of the process equipment. This was done only for the high-pressure pump, HEX, feed heater and gravity separator of the SCWD unit. The brine recovery section will be discussed in subsequent work. Calculations were performed assuming both ideal and non-ideal mixing (AP EoS) for a feed stream of 3.5 wt%. For the HEX calculations, the cold inlet temperature of 25 °C was taken and a heat exchange effectiveness (see Eq. (S.17) in the SI) of 90% was assumed with no heat loss.

The stream data can be found in the SI (Table S.4). From the data it was seen that the contribution of the excess enthalpy is minimal for the subcritical region and the SCW stream. However, in the supercritical region for NaCl concentrations of 3.5 wt% and greater the effect of the

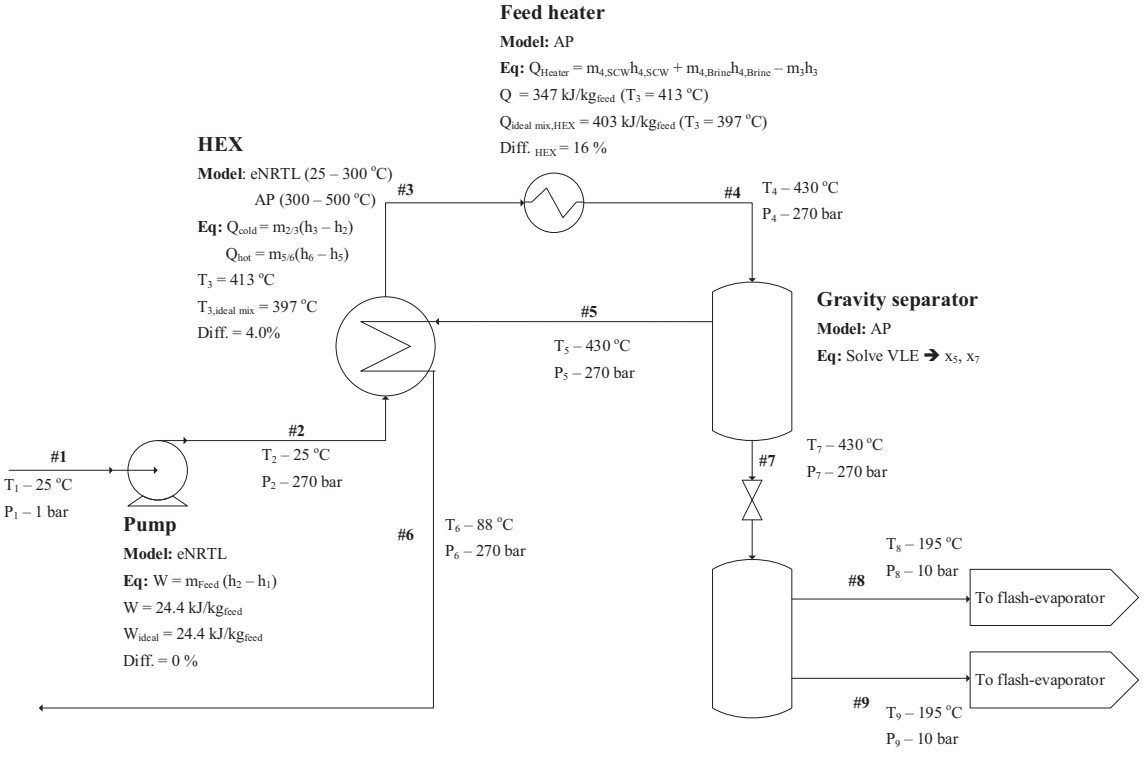

Fig. 6. SCWD process flow diagram with corresponding process unit equations.

non-ideal mixing enthalpy contribution to the total enthalpy becomes more pronounced (up to 44% for the brine stream). The main difference is observed for the HEX-heater section. For ideal mixing, the cold outlet temperature is under-predicted (as also shown in Section 3.3). If this under-predicted temperature is used to calculate the feed heater duty the value is comparable to that of the AP EoS determined duty. However, if the temperature is set to 413 °C the ideal mixing duty would be under-predicted (0.15 MJ_{th}/kg_{feed}). This is due to the heat of separation, which increases the feed heater duty. The calculation was also tested for a feed of 7 wt% NaCl. The cold outlet temperature was 393 °C (ideal mixing) and 416 °C (non-ideal mixing) and the subsequent calculated duty was 0.52 and 0.43 M_{Jth}/kg_{feed} (21% difference) for ideal and non-ideal mixing respectively. For 10 wt%, the difference between ideal (0.65 M_{Jth}/kg_{feed}) and non-ideal (0.50 M_{Jth}/kg_{feed}) increased to 30%, due to the effect of non-ideal mixing increasing with feed concentration. For concentrations higher than ± 10 wt%, the cold feed needs to be pre-heated before heat exchange due to a shift in pinch point (see Section 5.2) and the results for these feeds will be discussed in Section 5.4.

On a drinking water basis the feed heater duty (non-deal mixing basis) was 382, 528 and 668 $MJ/m^3_{drinking\ water}$ for a 3.5, 7 and 10 wt% feed, respectively. Odu et al. [18] calculated (using the Driesner correlations) the thermal energy requirement to be 450 $MJ_{th}/m^3_{drinking\ water}$ (feed of 3.5 wt% NaCl) to heat a 3.5 wt% feed from 415 to 460 °C at 300 bar. Lopez & Trembly [7] simulated a SCWD unit with chemical pre-treatment in Aspen Plus using the eNRTL model. The separation occurred at 430 °C and 221 bar and reasonable results could be obtained, however, when the pressure is further increased (to 270 bar) the discrepancies become significant. From the simulation, they estimated the energy consumption of the separator (solution was directly heated in the separator from 362 to 430 °C) to be 647–726 MJ_{th}/m^3_{feed} (variation is due to difference in pre-treatment step) for a 15.5 wt% feed stream. In a follow-up study Ogden & Trembly [8], experimentally investigated a pilot plant scale SCWD unit and determined (combination of experiments and Driesner correlations) the energy requirement to be between 389 and 495 kJ/kg (230–280 bar) for a 5 wt% and between 178 and 422 kJ/kg for a 18 wt% multicomponent feed. They also concluded that the eNRTL model was not sufficient in accurately determining results.

5.2. Composite curves

The effect of NaCl feed concentration on heat exchange and the remaining hot utility requirement (feed heater duty) was further investigated for higher concentration brines. Four feed concentrations typically found in industry were considered namely: 3.5 (seawater), 7.0 (reverse osmosis reject stream), 14 (mining/dairy industry) and 20 wt% NaCl (multi-effect evaporation feed stream). The cold inlet was set to 25 °C (3.5, 7.0 and 14 wt%) and hot outlet to 35 °C. The feed flow rate was set to 10 kg/h for all feeds and the pressure was set to 270 bar. The SCW (0.068 wt% NaCl) flow rates were calculated for separation temperature and pressure of 430 °C and 270 bar, with the values reported in the graphs. It was assumed that the pressure drop over the hot and cold side of the heat exchanger is negligible, which was in agreement with the experimental results. The cold curve for feed concentrations 3.5 and 7.0 wt% was shifted so that a minimum temperature difference (ΔT_{min}) of 10 °C was maintained at the pinch point. The composite curves for the four different feed concentrations are given in Fig. 7a–d. The minimum hot utility requirements are also reported in the graphs.

The results show that the hot utility requirement will decrease for higher feed concentrations due to the decrease in feed heat capacity. For higher feed concentrations, the pinch point shifts to the bottom of the composite curves namely, the inlet of the cold curve. This is due to the decrease in the SCW recovery becoming the dominating effect as opposed to the decrease in feed heat capacity. This will limit the heat exchange and lower the cold outlet temperatures for higher feed concentrations. To overcome the heat exchange limitation, the feed stream should be pre-heated before entering the heat exchanger. Pre-heating the feed will shift the pinch point to the higher temperature region. For a feed concentration of 14 wt%, the temperature difference at the inlet was marginally smaller (10 °C), than the temperature difference at the transition region (12 °C). Even though it seems as if the effect of pre-heating the feed and shifting the curves will be minimal, for the hot utility requirement, this will have a notable influence on the heat exchanger as will be seen in Section 5.3. For a feed concentration of 20 wt%, the feed was pre-heated to 200 °C and the cold curve was shifted closer to the hot curve (ΔT_{min} = 10 °C at the pinch point), as shown in Fig. 7d. By pre-heating the feed, the pinch point shifted back to the transition region of the SCW (higher temperature region). The required hot utility (to heat the feed to 430 °C) is 1.05 MJ/h, however, 5.60 MJ/h is also required to pre-heat the feed to 200 °C. 70% of this energy can be supplied by the remaining SCW energy (3.92 MJ/h) through stream splitting (see Section S.5.2 of the SI). The remaining heat can be supplied either by utility streams or other process streams such as brine waste streams.

From Fig. 7d, it can also be seen that the cooling requirement for the SCW stream will increase. From the composite curve the cooling requirement is estimated to be 4.01 MJ/h. However, when referring to the stream splitting scheme in the SI, it is seen that the SCW is cooled to 38 °C and thus the further cooling requirement is minimal. Additionally, the SCWD unit would most likely be integrated with another process, as a brine waste treatment step, for which the SCW stream could also serve as a utility stream and further cooling would not be required.

Increasing the separation pressure will also have an effect, as the critical point (where the pinch point is usually located) is shifted to a higher temperature region. Increasing the separation pressure (constant separation temperature) increases the pseudocritical temperature (similar to the effect of salt addition) and the latent heat, required for phase transition, becomes more distributed over a certain temperature interval [35]. The composite curves for a 3.5 wt% NaCl feed at 250, 270 and 300 bar are given in Fig. 8. The cold curve was shifted so that ΔT_{min} is equal to 10 °C at the pinch point.

The minimum required heat utility will decrease, however, the drawback of increasing the pressure is that the quality of SCW will decrease (higher NaCl concentration) as well as the recovery. The separation temperature would have to be increased once more to reach the specified requirements. Increasing the feed concentration will also decrease the SCW recovery, but the NaCl concentration of the SCW will remain the same as this is only a function of separation temperature and pressure. Overall when comparing the change in the minimum hot utility requirement for feed concentration and pressure, it is seen that feed concentration has a greater influence on the heat exchange potential.

5.3. SCWD HEX and feed heater

Heat recovery plays an important role in making the energy intensive process viable. As shown above, heat from the SCW stream is utilised to heat the feed stream before it is further heated in the feed heater, which is the main energy consumer of the process. Higher cold (feed) stream outlet temperatures at the HEX will translate into a lower energy requirement for the heater and can be achieved by increasing the heat exchange area of the HEX. There is, however, a trade-off that needs to be made between the size of the heat exchanger (capital costs) and the cost of energy for the feed heater (operational costs). The trade-off between heat exchange and feed heater energy duty is compared in Fig. 9. The HEX cold outlet temperature is plotted as a function of the $U.A/m_{feed}$ value for different feed concentrations, while the feed heater duty, as an indicator for the operational costs, is also shown. The $U.A$ were calculated by using counter-current heat exchanger equations assuming no heat loss (See Section S.3.3 in the SI). The pressure was set to 270 bar and the hot inlet temperature to 430 °C, while the HEX

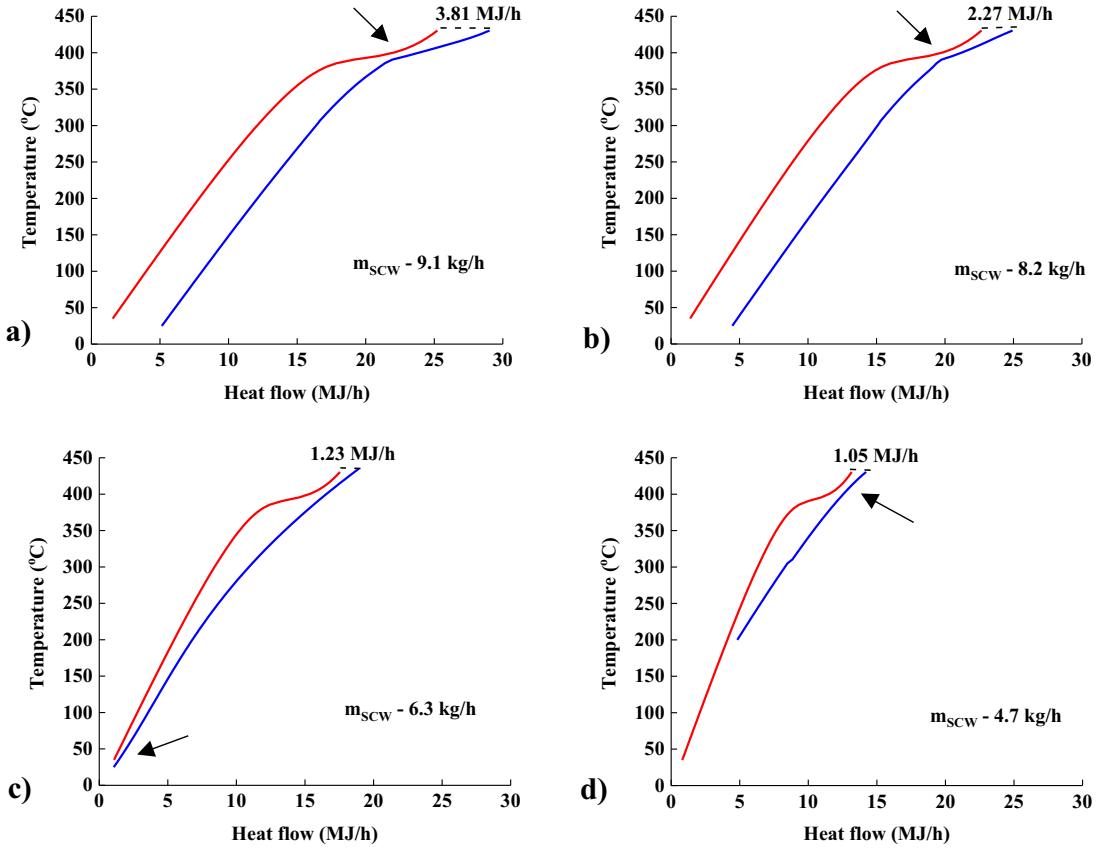

Fig. 7. Composite curves and hot utility requirement for different feed concentrations of NaCl for a feed rate of 10 kg/h a) 3.5 wt% b) 7 wt% d) 14 wt% c) 20 wt% (Arrow – pinch point; ■ Hot stream (SCW); ■ Cold stream (Feed)).

effectiveness (and consequently the hot outlet temperature) was varied. Originally the cold inlet temperature was set to 25 °C for all feed concentrations. However, for higher feed concentrations (> 14 wt% NaCl) the heat transfer becomes limited at the cold feed inlet side (see Section 5.2). The feed is pre-heated to 100 °C for 14 wt% and 200 °C for 20 wt%. For these temperatures the pinch point is once more in the high temperature region. The feed heater duty covers the heating of the HEX cold stream from the outlet temperature to the separation temperature (430 °C) as well as the separation between the SCW and the concentrated brine phase (see Eq. (S.20) in the SI). The HEX pre-heater duty of the feed is not shown in the graph but mentioned in the caption of Fig. 9.

In the SI (Section S.5.3) the $U.A/m_{feed}$ values can be found for the case when the cold inlet temperature is 25 °C for all feeds. In that case the cold outlet temperature for the 20 wt% feed was not > 340 °C due to the pinch point being at the cold inlet side. From Fig. 9, it is seen that a $U.A/m_{feed}$ value between 20 and 25 kJ/kg·K would be the best compromise between the duty of the feed heater and the HEX size. Between 20 and 25 kJ/kg·K, the rate of decrease in feed heater duty is lower, especially for 20 wt%, and a larger HEX size will not significantly reduce the energy consumption of the feed heater.

From the simulation results of Lopez & Trembly [7], the $U.A/m_{feed}$ values were calculated for their feed HEX, assuming an overall heat transfer coefficient of 1500 W/m^{2}K. The calculated values were 12 and 14 kJ/kg·K (varied with pre-treatment) for a 15.5 wt% multicomponent feed. The values are lower than the range selected in Fig. 9, however, the outlet temperature for their HEX was also lower, being 362 °C for both cases.

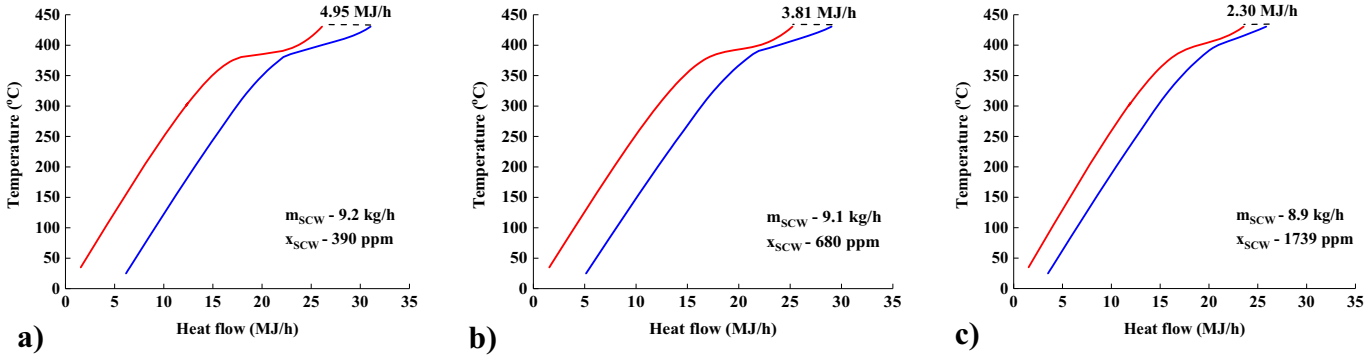

Fig. 8. Composite curves and hot utility requirement for different separation pressures of 3.5 wt% NaCl feed a) 250 bar b) 270 bar c) 300 bar. (■ Hot stream (SCW); ■ Cold stream (Feed)).

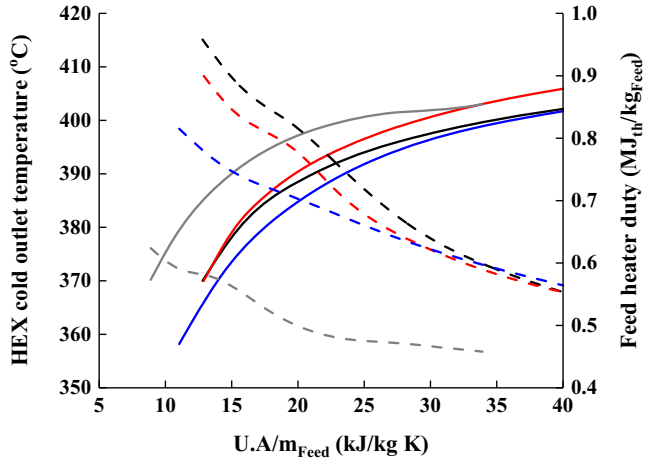

Fig. 9. Outlet temperature of cold stream from HEX and feed heater duty as a function of the HEX size parameter U.A/m_{feed} for different feed concentration (solid – HEX cold stream outlet temperature; dashed – feed heater duty; ■ 3.5 wt%; ■ 7 wt%; ■ 14 wt% (HEX pre-heater duty: 0.026 MJ_{th}/kg_{feed}); ■ 20 wt % (HEX pre-heater duty: 0.17 MJ_{th}/kg_{feed})).

5.4. Total SCWD energy consumption

An overview of the total energy consumption of the SCWD for the four different concentrations is given in Table 1. A $U.A/m_{feed}$ value of 20 kJ/kg K (see Fig. 9) was selected for the calculation of the feed heater duty. The separation conditions were set to 430 °C and 270 bar, and the 14 and 20 wt% feeds were first pre-heated from 25 °C to 100 and 200 °C, respectively.

When comparing the results in Table 1, it can be seen that the overall energy consumption of the SCWD process decreases with increased feed concentration when based on the amount of brine fed. This is attributed to the lower heat capacity which 1) leads to improved heat exchange potential inside the HEX, allowing for higher cold (feed) outlet temperatures, and 2) directly lowers the energy requirement of the feed heater. For a feed concentration of 14 wt% the feed heater inlet temperature is lower than for 7 wt%, however, due to the decrease in the heat capacity the heater duty and total energy consumption is still below that of a 7 wt% feed.

Another advantage of having a higher concentration feed is that the energy requirement can be divided between high – and low quality heat (temperature). For lower concentration feeds, only high quality energy from *e.g.* fired heaters will be needed to heat the feed to supercritical conditions. On the other hand, for more concentrated feeds (> 7 wt% NaCl), only a fraction of the total energy requirement needs to be supplied by fired heaters (high quality expensive energy), the rest can be supplied by utilities such as steam (lower quality, less expensive energy). This will be reflected in the capital and operational costs of the SCWD unit.

On a drinking water basis the energy consumption of the SCWD process will increase with feed concentration, which is due to the reduction in the SCW recovery. This shows that SCWD is better suited for the treatment of waste brine streams, rather than the production of drinking water from low saline feeds.

6. Conventional ZLD comparison

Conventional ZLD processes usually consists of multiple process units, which can be divided into two steps namely the brine concentration step and the crystallisation step. Brine concentration is usually done using mechanical vapour compressor (MVC) brine concentrators or thermal concentrators. Membranes are sometimes also used, however, for this section only thermal/mechanical units are discussed. Crystallisation is usually done through evaporation of the water (Evaporative crystallisation – EC), although eutectic freeze crystallisation (EFC) is also sometimes applied. In Table 2 the energy consumption of the different units is summarised.

Upon comparing the energy consumption of the units to that of SCWD (Table 1) it is seen that SCWD has a higher energy consumption than for the conventional ZLD standalone units. When looking at the energy consumption of a complete ZLD process (energy requirement of brine concentrator and crystalliser together) the total energy requirement is 0.37 MJ_{th}/kg_{feed} [37] and 0.51–0.63 MJ_{th}/kg_{feed} [38]. Compared to the values in Table 1, the energy requirement of SCWD is still higher as a standalone unit. However, if the process were to be integrated as a post-treatment step for another process, the energy consumption could be further reduced, as these streams will already be partly heated and pressurised. Energy can also be retrieved from the ZLD section of the unit (stream 12, Fig. 1) and used to pre-heat the feed stream for higher concentration feeds.

7. Conclusions

The influence of NaCl feed concentration on the energy consumption of SCWD was investigated both experimentally and theoretically. Validation with both experimental pilot plant results and literature data showed that the AP EoS was able to accurately predict phase equilibria measurements in the supercritical region. Compared to an ideal mixing approach, the AP EoS was superior in predicting the enthalpies. The experimentally measured cold outlet temperatures of the pilot plant feed-SCW HEX, showed that for feed concentrations of 1.0 to 7.0 wt% NaCl, the reduction in the feed heat capacity had the dominating effect (as opposed to the decrease in the SCW recovery). The heat exchange potential increased with feed concentration, as evident from the increase in the measured cold outlet temperatures. For higher feed concentrations (> 7 wt%) the reduction in SCW recovery became significant enough that the pinch point of the composite curves shifted to the lower temperature region. This resulted in lower cold (feed) outlet

Table 1
Total SCWD energy consumption for four feed stream concentrations for $U.A/m_{feed}$ = 20 kJ/kg K.

Feed concentration (wt %)	Pump duty[a] (MJ_{th}/kg_{feed})	Pre-heating of feed (MJ_{th}/kg_{feed})[b]	Feed heater inlet temperature (°C)	Feed heater duty[a] (MJ_{th}/kg_{feed})	Overall energy consumption[c] (MJ_{th}/kg_{feed})	Overall energy consumption[c] ($MJ_{th}/kg_{drinking\ water}$)
3.5	0.048	–	389	0.81	0.90	0.99
7.0	0.046	–	390	0.78	0.83	1.01
14	0.042	0.026[d]	385	0.70	0.77	1.22
20	0.039	0.17[e]	397	0.50	0.71	1.51

[a] Thermal energy requirement (50% efficiency).
[b] Energy supplied by SCW stream is subtracted.
[c] Sum of thermal energy of pump, pre-heater and feed heater.
[d] Heated to 100 °C.
[e] Heated to 200 °C.

Table 2
Comparison of the energy consumption for conventional ZLD units.

ZLD unit	Feed concentration (wt%)	Reported energy consumption	Converted thermal energy consumption[a]	Reference
1st step: Brine concentration				
MVC	4.5–8.0	28–39 kWh_{elec}/m^3_{feed}	0.2–0.28 MJ_{th}/kg_{feed}	[36]
MVC	10	18.5 kWh_{elec}/m^3_{feed}	0.13 MJ_{th}/kg_{feed}	[37]
MVC	0.4–1.2	20–25 kWh_{elec}/m^3_{feed}	0.14–0.18 MJ_{th}/kg_{feed}	[38]
2nd step: Crystallisation				
EC	Saturation	33.9 kWh_{elec}/m^3_{feed}	0.24 MJ_{th}/kg_{feed}	[37]
EC	Saturation	52–66 kWh_{elec}/m^3_{feed}	0.37–0.45 MJ_{th}/kg_{feed}	[38]
EFC	4	22.9 kWh_{elec}/m^3_{feed} – 1st crystalliser 0.10 MJ_{th}/kg_{feed} – 2nd crystalliser	0.16 MJ_{th}/kg_{feed} – 1st crystalliser 0.10 MJ_{th}/kg_{feed} – 2nd crystalliser	[39]

[a] Assuming an efficiency of 50% to convert the thermal energy to electrical.

temperatures for the HEX. Pre-heating the feed prior to the HEX shifted the pinch point to the higher temperature region once more, which assisted with improving heat exchange potential. Theoretical results showed that for higher separation pressures, the heat exchange potential also improved as evident from the calculated minimum hot utility requirement of the composite curves. Increasing the pressure, however, increased the NaCl concentration of the SCW stream and decreased the SCW recovery (higher feed concentration also decreased the recovery). The calculated overall SCWD energy consumption decreased with feed concentration. This is due to the lowered heat capacity, which contributed to improving the heat exchange potential in the HEX and also directly lowering the energy requirement of the feed heater. The energy requirement for higher concentrations can be divided between low quality energy (pre-heating the HEX feed) and high-quality energy (reaching separation temperature) as opposed to only high quality (temperature) energy required for lower concentration feeds.

Declaration of competing interest

We the authors that we have no significant competing financial, professional, or personal interests that might have influenced the performance or presentation of the work described in this manuscript.

Acknowledgements

This work was performed in the cooperative framework of Wetsus, European Centre of Excellence for Sustainable Water Technology (www.wetsus.nl). Wetsus is co-funded by the Dutch Ministry of Economic Affairs and Ministry of Infrastructure and Environment, the European Union Regional Development Fund, the Province of Fryslân and the Northern Netherlands Provinces. This work is part of a project that has received funding from the European Union's Horizon 2020 research and innovation programme under the Marie Skłodowska-Curie grant agreement No. 665874. The authors would like to thank the participants of the research theme “Desalination” for the fruitful discussions and their financial support. The authors would like to thank Dr. Andrzej Anderko for sharing his original FORTRAN code to assist with some of the calculations. The authors would also like to thank Benno Knaken and Johan Agterhorst for their valuable contribution to the maintenance of the pilot plant.

Appendix A. Supplemenatry data

References

[1] E. Jones, M. Qadir, M.T.H. van Vliet, V. Smakhtin, S. mu Kang, The state of desalination and brine production: a global outlook, Sci. Total Environ. 657 (2019) 1343–1356, https://doi.org/10.1016/j.scitotenv.2018.12.076.
[2] V.G. Gude, Desalination and sustainability - an appraisal and current perspective, Water Res. 89 (2016) 87–106, https://doi.org/10.1016/j.watres.2015.11.012.
[3] A. Giwa, V. Dufour, F. Al Marzooqi, M. Al Kaabi, S.W. Hasan, Brine management methods: recent innovations and current status, Desalination 407 (2017) 1–23, https://doi.org/10.1016/j.desal.2016.12.008.
[4] D. Xevgenos, K. Moustakas, D. Malamis, M. Loizidou, An overview on desalination & sustainability: renewable energy-driven desalination and brine management, Desalin. Water Treat. 57 (2016) 2304–2314, https://doi.org/10.1080/19443994.2014.984927.
[5] T. Tong, M. Elimelech, The global rise of zero liquid discharge for wastewater management: drivers, technologies, and future directions, Environ. Sci. Technol. 50 (2016) 6846–6855, https://doi.org/10.1021/acs.est.6b01000.
[6] S. van Wyk, S.O. Odu, A.G.J. van der Ham, S.R.A. Kersten, Design and results of a first generation pilot plant for supercritical water desalination (SCWD), Desalination 439 (2018), https://doi.org/10.1016/j.desal.2018.03.028.
[7] D.E. López, J.P. Trembly, Desalination of hypersaline brines with joule-heating and chemical pre-treatment: conceptual design and economics, Desalination 415 (2017) 49–57, https://doi.org/10.1016/j.desal.2017.04.003.
[8] D.D. Ogden, J.P. Trembly, Desalination of hypersaline brines via joule-heating: experimental investigations and comparison of results to existing models, Desalination 424 (2017) 149–158, https://doi.org/10.1016/j.desal.2017.10.006.
[9] S.J. Metz, I. Leusbrock, Method and System for Supercritical Removal of an Inorganic Compound, US 2011/0180384 A1 (2011).
[10] F.J. Armellini, J.W. Tester, Experimental methods for studying salt nucleation and growth from supercritical water, J. Supercrit. Fluids 4 (1991) 254–264, https://doi.org/10.1016/0896-8446(91)90020-7.
[11] M. Hodes, P.A. Marrone, G.T. Hong, K.A. Smith, J.W. Tester, Salt precipitation and scale control in supercritical water oxidation - part a: fundamentals and research, J. Supercrit. Fluids 29 (2004) 265–288, https://doi.org/10.1016/S0896-8446(03)00093-7.
[12] F.J. Armellini, J.W. Tester, Solubility of sodium chloride and sulfate in sub- and supercritical water vapor from 450–550 °C and 100–250 bar, Fluid Phase Equilib. 84 (1993) 123–142, https://doi.org/10.1016/0378-3812(93)85120-B.
[13] I. Leusbrock, S.J. Metz, G. Rexwinkel, G.F. Versteeg, The solubilities of phosphate and sulfate salts in supercritical water, J. Supercrit. Fluids 54 (2010) 1–8, https://doi.org/10.1016/j.supflu.2010.03.003.
[14] I. Leusbrock, S.J. Metz, G. Rexwinkel, G.F. Versteeg, Solubility of 1:1 alkali nitrates and chlorides in near-critical adn supercritical water, J. Chem. Eng. Data 54 (2009) 3215–3223.
[15] M. Schubert, J.W. Regler, F. Vogel, Continuous salt precipitation and separation from supercritical water. Part 1: type 1 salts, J. Supercrit. Fluids 52 (2010) 99–112, https://doi.org/10.1016/j.supflu.2009.10.002.
[16] M. Schubert, J.W. Regler, F. Vogel, Continuous salt precipitation and separation from supercritical water. Part 2. Type 2 salts and mixtures of two salts, J. Supercrit. Fluids 52 (2010) 113–124, https://doi.org/10.1016/j.supflu.2009.10.003.
[17] M. Schubert, J. Aubert, J.B. Muller, F. Vogel, Continuous salt precipitation and separation from supercritical water. Part 3: interesting effects in processing type 2 salt mixtures, J. Supercrit. Fluids 61 (2012) 44–54, https://doi.org/10.1016/j.supflu.2011.08.011.
[18] S.O. Odu, A.G.J. Van Der Ham, S. Metz, S.R.A. Kersten, Design of a process for supercritical water desalination with zero liquid discharge, Ind. Eng. Chem. Res. 54 (2015) 5527–5535, https://doi.org/10.1021/acs.iecr.5b00826.
[19] J.E. Miller, Review of water resources and desalination techniques, Sand Rep. (2003) 1–54 (doi:SAND 2003-0800).
[20] J. Gmehling, B. Kolbe, M. Kleiber, J. Rarey, Chemical Thermodynamics for Process Simulation, (2013).
[21] M. Holmgren, XSteam - IAPWS IF-97, (2007).
[22] A. Anderko, K.S. Pitzer, Equation-of-state representation of phase equilibria and volumetric properties of the system NaCl-H2O above 573 K, Geochim. Cosmochim. Acta 57 (1993) 1657–1680, https://doi.org/10.1016/0016-7037(93)90105-6.
[23] J.J. Kosinski, A. Anderko, Equation of state for high-temperature aqueous electrolyte and, Fluid Phase Equilib. 183–184 (2000) 75–86.
[24] M.D. Bermejo, A. Martín, L.J. Florusse, C.J. Peters, M.J. Cocero, The influence of Na2SO4 on the CO2 solubility in water at high pressure, Fluid Phase Equilib. 238 (2005) 220–228, https://doi.org/10.1016/j.fluid.2005.10.006.
[25] M.D. Bermejo, A. Martin, M.J. Cocero, Application of the Anderko-Pitzer EoS to the calculation of thermodynamical properties of systems involved in the supercritical water oxidation process, J. Supercrit. Fluids 42 (2007) 27–35, https://doi.org/10.1016/j.supflu.2007.01.011.
[26] T. Driesner, C.A. Heinrich, The system H2O-NaCl. Part I: correlation formulae for

phase relations in temperature-pressure-composition space from 0 to 1000 C, 0 to 5000 bar, and 0 to 1 XNaCl, Geochim. Cosmochim. Acta 71 (2007) 4880–4901, https://doi.org/10.1016/j.gca.2006.01.033.
[27] T. Driesner, The system H2O-NaCl. Part II: correlations for molar volume, enthalpy, and isobaric heat capacity from 0 to 1000 °C, 1 to 5000 bar, and 0 to 1 XNaCl, Geochim. Cosmochim. Acta 71 (2007) 4902–4919, https://doi.org/10.1016/j.gca.2007.05.026.
[28] M. Chase, C. Davies, J.R. Downey, D.J. Frurip, R.A. McDonald, A.N. Syverud, JANAF thermochemical tables third edition - part I, Al-co, J. Phys. Chem. Ref. Data 14 (1985).
[29] J.M.H. Levelt Sengers, Dilute mixtures and solutions near critical points, Fluid Phase Equilib. 30 (1986) 31–39, https://doi.org/10.1016/0378-3812(86)80038-3.
[30] Y. Song, C.-C. Chen, Symmetric Electrolyte Nonrandom Two-liquid Activity Coefficient Model, (2009), pp. 7788–7797, https://doi.org/10.1021/ie9004578.
[31] Y. Yan, C.C. Chen, Thermodynamic representation of the NaCl + Na2SO4 + H2O system with electrolyte NRTL model, Fluid Phase Equilib. 306 (2011) 149–161, https://doi.org/10.1016/j.fluid.2011.03.023.
[32] K.S. J.C. Tanger Pitzer, Thermodynamics of NaCl-H2O a new equation of state for the near critical region and comparisions with other equations for adjoining regions, Geochim. Cosmochim. Acta 53 (973–98) (1989) 973–987.
[33] J.L. Bischoff, R.J. Rosenbauer, An emperical equation of state for hydrothermal seawater (3.2 percent NaCl), Am. J. Sci. 285 (1985) 725–763.
[34] C. Palliser, R. Mckibbin, A model for deep geothermal Brines, III: thermodynamic properties – enthalpy and viscosity, Transp. Porous Media 33 (1998) 155–171, https://doi.org/10.1023/a:1006549810989.
[35] D.T. Banuti, M. Raju, P.C. Ma, M. Ihme, Seven questions about supercritical fluids – towards a new fluid state diagram, 55th AIAA Aerosp. Sci. Meet., Grapevine, 2017, pp. 1–15, , https://doi.org/10.2514/6.2017-1106.
[36] R.L. Mcginnis, N.T. Hancock, M.S. Nowosielski-slepowron, G.D. Mcgurgan, Pilot demonstration of the NH 3/CO2 forward osmosis desalination process on high salinity brines, Desalination 312 (2013) 67–74, https://doi.org/10.1016/j.desal.2012.11.032.
[37] B. Ericsson, B. Hallmans, Treatment of saline wastewater for zero discharge at the Debiensko coal mines in Poland, Desalination 105 (1996) 115–123.
[38] M. Mickley, Survey of High-Recovery and Zero Liquid Discharge Technologies for Water Utilities, (2008).
[39] M.J. Fernandez-Torres, D.G. Randall, R. Melamu, H. Von Blottnitz, A comparative life cycle assessment of eutectic freeze crystallisation and evaporative crystallisation for the treatment of saline wastewater, Desalination 306 (2012) 17–23, https://doi.org/10.1016/j.desal.2012.08.022.

Nomenclature

AP: Anderko & Pitzer
EC: Evaporative crystallisation
EFC: Eutectic freeze crystallisation
eNRTL: Electrolyte non-random two liquids
EoS: Equation of state
HEX: Heat exchanger
IAPWS IF-97: International Association for Properties of Water and Steam Industrial Formulation 1997
MVC: Mechanical vapour compressor
SCW: Supercritical water
SCWD: Supercritical water desalination
SI: Supporting information
VLE: Vapour liquid equilibrium
ZLD: Zero liquid discharge

Symbols

a: Helmholtz free energy
A: Area
C_p*:* Specific isobaric heat capacity
h: Enthalpy
ΔH_{diss}*:* Enthalpy of dissociation
$\dot{m}$*:* Mass flow
P: Pressure
$\dot{Q}$*:* Duty
R: Gas constant
T: Temperature
U: Overall heat transfer coefficient
v: Molar volume
W: Work
x: Mass fraction
X: Mole fraction

Greek symbols

γ*:* Activity coefficient
κ_{TX}*:* Isothermal compressibility factor

Sub-/superscript

ex: Excess
dip: Dipolar
i: Initial/species *i*
min: Minimum
per: Perturbation
ref: Reference
rep: Repulsive
res: Residual
SC: Supercritical
sub: Subcritical